

Facile Fabrication of Redox-Active and Electrochromic Poly(amide-amine) Films Through Electrochemical Oxidative Coupling of Arylamino Groups

Sheng-Huei Hsiao, Hui-Min Wang

Department of Chemical Engineering and Biotechnology, National Taipei University of Technology, Taipei 10608, Taiwan
Correspondence to: S.-H. Hsiao (E-mail: shhsiao@ntut.edu.tw)

Received 17 February 2016; accepted 17 March 2016; published online 00 Month 2016

DOI: 10.1002/pola.28124

ABSTRACT: Two novel electropolymerizable monomers, namely 3,5-bis(4-diphenylaminobenzamido)-*N*-[4-(carbazol-9-yl)phenyl]benzamide (**5**) and 3,5-bis(4-diphenylaminobenzamido)-*N*-[4-(3,6-dimethoxycarbazol-9-yl)phenyl]benzamide (**5-MeO**), were synthesized, and their electrochemical properties were studied by cyclic voltammetry. The electron-withdrawing amide groups efficiently blocked the radical cations delocalization between the two terminal TPA groups, rendering the electropolymerization of the TPA groups feasible. The polymer electrodeposited from monomer **5** could be further crosslinked through electrocoupling of the carbazole groups, which showed both electro-

chromic and fluorescent properties (the emission of blue light (460 nm) in solid state). Both of the electro-generated polymer films derived from **5** and **5-MeO** showed reversible electrochemical oxidation processes in the range of 0–1.4 V with strong color changes and high contrast ratios in the visible and NIR regions upon electro-oxidation. © 2016 Wiley Periodicals, Inc. *J. Polym. Sci., Part A: Polym. Chem.* **2016**, *00*, 000–000

KEYWORDS: carbazole; electrochemistry; fluorescence; poly(amide-amine)s; redox polymers; triphenylamine

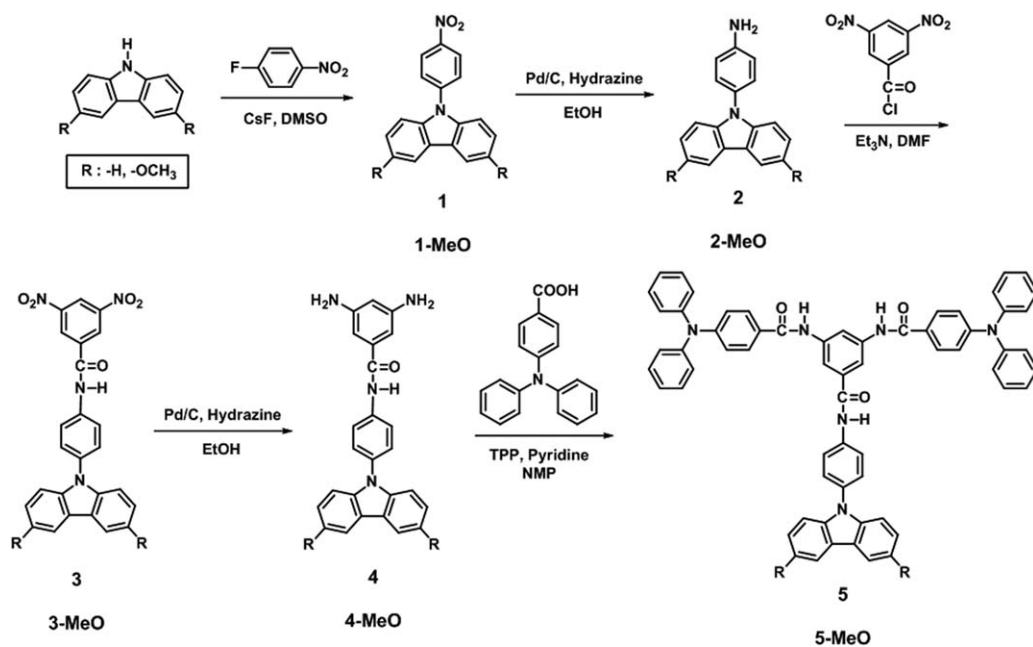
INTRODUCTION Electrochromism involves the process of changing the absorption profile of a material with application of an electric field or passing of electrical charge.¹ This interesting property led to the development of many technological applications such as smart windows,² color changing eyewear,³ display devices,⁴ and military camouflage.⁵ Recent high-profile commercialization of electrochromic materials includes the Boeing 787 Dreamliner windows manufactured by Gentex.⁶ Up to now, many organic and inorganic materials have been developed for electrochromic applications, such as inorganic metal oxide, mixed-valence metal complexes, organic small molecules, and conjugated polymers.⁷ Among the many different kinds of electrochromic materials available, electrochromic conjugated polymers have received tremendous attention due to their fine-tuning of coloration, high coloration efficiency, fast switching speeds, high contrast ability, and good processability.⁸

Arylamine-based derivatives have attracted significant attention in the past years due to their unique properties that allow them to have potential applications in organic electronics, photonics and magnetic materials.⁹ Most of the hole-transporting materials contain triarylamine moieties in their molecular structures.¹⁰ Many star-shaped, dendrimeric and polymeric triarylamines have been synthesized as photocon-

ductors and hole-transporting materials for various electro-optical applications.¹¹ Due to the good electron-donating nature of triarylamines, their derived oligomers and polymers have been widely studied as hole-transporting materials for a number of applications, such as xerography, organic field-effect transistors, photovoltaics, organic light-emitting devices, and so forth.^{9–11} In addition, the application of redox-active polymers as active electrode materials has attracted much attention in the area of secondary battery research during the past few decades.¹² For example, redox-active polytriphenylamine¹³ and poly(*N*-vinylcarbazole)¹⁴ have been evaluated as cathode active materials for use in rechargeable lithium batteries.

Molecules containing electroactive carbazole and triphenylamine (TPA) moieties are interesting materials because their redox and photophysical properties make them suitable for use as hole carriers in optoelectronic devices.¹⁰ In the past decade, a huge amount of high-performance polymers (typically, aromatic polyamides and polyimides) carrying the TPA and/or carbazole unit have been prepared and evaluated for electrochromic applications.¹⁵ It is well known that the one-electron oxidation of unsubstituted TPA causes the generation of reactive radical cations, which typically undergo irreversible dimerization to tetraphenylbenzidine (TPB) as a

© 2016 The Authors. *Journal of Polymer Science Part A: Polymer Chemistry* Published by Wiley Periodicals, Inc.
This is an open access article under the terms of the Creative Commons Attribution License, which permits use, distribution and reproduction in any medium, provided the original work is properly cited.



SCHEME 1 Synthetic route to star-shaped monomers **5** and **5-MeO**.

result of oxidative coupling.¹⁶ The dimerization occurs exclusively in the para position to the nitrogen centers, that is, the sites with the highest spin electron density. In general, the TPA dimerization reaction does not extend into a polymerization process because of the relatively higher stability of TPB radical cation.¹⁷ The introduction of a nonconjugated spacer or an electron-deficient group, such as amide, imide, or oxadiazole units between the two TPA groups, however, increases the dimerization reactivity of the TPA radical cation, allowing individual TPA to realize an independent coupling reaction and rendering the electropolymerization process feasible.¹⁸ Similarly, as reported by Ambrose and coworkers in their pioneering work¹⁹ devoted to anodic oxidation of carbazole and various *N*-substituted carbazoles, ring–ring coupling is the predominant decay pathway, the carbazole radical cation yielding 3,3'-bicarbazyls. Although these bicarbazyls possess a lower first oxidation potential than the corresponding monomers and are therefore, potentially, more suitable for electrochemical polymerization, dimers were cleanly obtained in quantitative yields, because of the high stability of the oxidized states (bicarbazyl cations).²⁰ Polymerization may occur anodically by using bis(carbazole)s, *N*-linked by a spacer, to produce materials with redox properties characteristic to bicarbazyls.²¹

Electrochemical polymerization provides the unique advantage to combine both synthesis and direct fabrication of electroactive polymer films on the electrode surface. This procedure significantly shortens the experimental time and avoids the solubility issues often encountered with conventional chemical methods, thus enlarging the scope of candidate polymers for electrochromic applications. As a continuation of our recent efforts in developing electrochromic materials by electrochemical synthesis, herein we design and synthesize a novel electropolymerizable star-shaped monomer **5** (Scheme 1) featuring

an 1,3,5-trisubstituted benzene ring as an interior core bridged by amide linkages terminal electroactive TPA and carbazole units. In addition to the polymer formed through TPA dimerization of monomer **5**, the presence of the carbazole moiety would lead to further electrochemical crosslinking process. For a comparative study, an analogous star-shaped molecule **5-MeO** with methoxy groups substituted on the active C-3 and C-6 sites of the carbazole unit was also synthesized, and its electrochemical behavior was investigated. Both of the electro-generated poly(amide-amine) films from monomers **5** and **5-MeO** displayed fluorescent and electrochromic properties. This work provides a model to design star-shaped monomers capable to form electrochemically active polymers with potential applications in electronic and optoelectronic devices.

EXPERIMENTAL

Materials

As shown in Scheme 1, the diamino compounds *N*-(4-(carbazol-9-yl)phenyl)-3,5-diaminobenzamide (**4**) (mp = 237–238 °C) and *N*-[4-(3,6-dimethoxycarbazol-9-yl)phenyl]-3,5-diaminobenzamide (**4-MeO**) (mp = 238–239 °C) were synthesized according to a literature method.²² The synthetic details and their characterization data have been reported in our previous publications.²³ 4-Carboxytriphenylamine was synthesized by the cesium fluoride (CsF)-mediated *N*-arylation reaction of diphenylamine with *p*-fluorobenzonitrile, followed by the alkaline hydrolysis of the intermediate 4-cyanotriphenylamine.²⁴ *N*-(4-Aminophenyl)carbazole was prepared by the fluoro-displacement of *p*-fluoronitrobenzene with carbazole in the presence of CsF in dimethyl sulfoxide (DMSO), followed by Pd/C-catalyzed hydrazine reduction of the intermediate *N*-(4-nitrophenyl)carbazole.²⁴ Tetrabutylammonium perchlorate (Bu₄NClO₄, TCl) was recrystallized twice from ethyl acetate

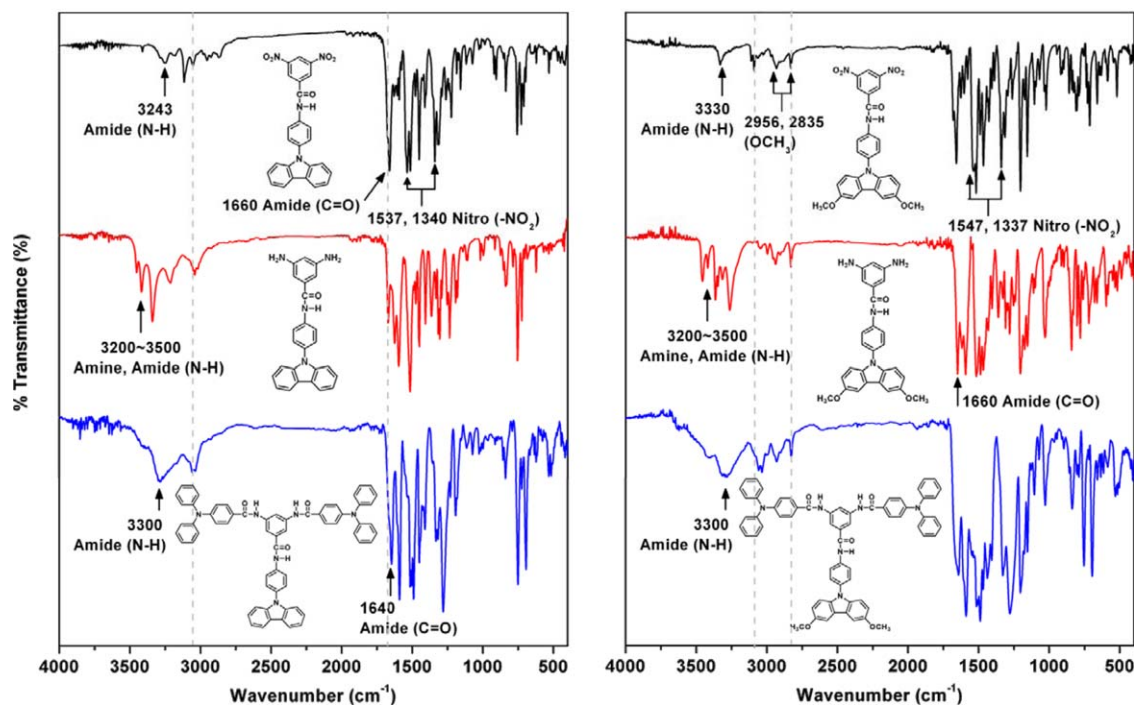
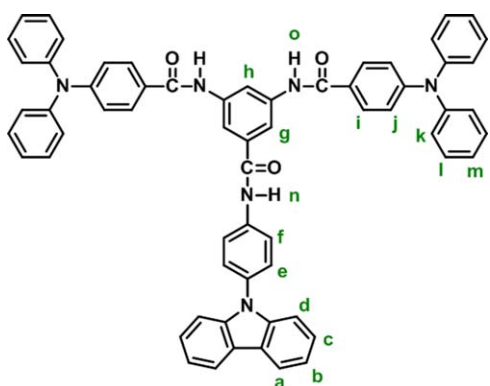


FIGURE 1 IR spectra of the synthesized compounds. [Color figure can be viewed in the online issue, which is available at wileyonlinelibrary.com.]

and then dried *in vacuo* before use. All other solvents and reagents were used as received from commercial sources.

Synthesis of Star-Shaped Monomers **5** and **5-MeO** *N*-(4-(Carbazol-9-yl)Phenyl) [3,5-Bis (4-Diphenylaminobenzamido)]Benzamide (**5**)

In a 50-mL round-bottom flask equipped with a stirring bar, a mixture of 0.275 g (0.7 mmol) of diamino compound **4**, 0.424 g (1.5 mmol) of 4-carboxytriphenylamine, 0.7 mL of triphenyl phosphite (TPP), 0.25 mL of pyridine, and 1 mL of NMP was heated with stirring at 120 °C for 3 h. The solution was poured slowly with stirring into 150 mL of methanol to precipitate white product. The precipitated product was collected by filtration, washed repeatedly with methanol and



Structure 1. [Color figure can be viewed in the online issue, which is available at wileyonlinelibrary.com.]

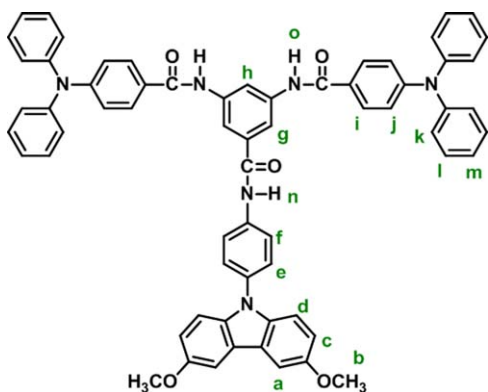
hot water, and dried to give 0.65 g of the desired monomer **5** as white powder in 99% yield.

IR (KBr): 3300 cm^{-1} (amide N – H stretching); 1640 cm^{-1} (amide C = O stretching). ^1H NMR (500 MHz, CDCl_3 , δ , ppm): 6.94 (d, $J = 8.5$ Hz, 4H, H_i), 7.09 (m, 12H, $H_m + H_k$), 7.26 (m, 12H, $H_b + H_d + H_j$), 7.35 (t, $J = 9.0$ Hz, 2H, H_c), 7.45 (d, $J = 8.5$ Hz, 2H, H_e), 7.68 (d, $J = 8.5$ Hz, 4H, H_l), 7.96 (two overlapped doublets, 4H, $H_f + H_g$), 8.13 (d, $J = 7.5$ Hz, 2H, H_a), 8.27 (s, 1H, H_h), 8.59 (s, 2H, amide H_o), 9.37 (s, 1H, amide H_n). Anal. Calcd. for $\text{C}_{63}\text{H}_{46}\text{N}_6\text{O}_3$ (935.09): C, 80.92%; H, 4.96%; N, 8.99%. Found: C, 80.55%; H, 4.93%; N, 8.90%.

N-(4-(3,6-Dimethoxycarbazol-9-yl)Phenyl) [3,5-Bis (4-Diphenylaminobenzamido)]Benzamide (**5-MeO**)

In a 50-mL round-bottom flask equipped with a stirring bar, a mixture of 0.317 g (0.7 mmol) of diamino compound **4-MeO**, 0.434 g (1.5 mmol) of 4-carboxytriphenylamine, 0.70 mL of triphenyl phosphite (TPP), 0.25 mL of pyridine, and 1 mL of NMP was heated with stirring at 120 °C for 3 h. The solution was poured slowly with stirring into 150 mL of methanol to precipitate white product. The precipitated product was collected by filtration, washed repeatedly with methanol and hot water, and dried to give 0.64 g of the desired monomer **5-MeO** as white powder in 92% yield.

IR (KBr): 3330 cm^{-1} (amide N – H stretching); 1640 cm^{-1} (amide C = O stretching). ^1H NMR (500 MHz, CDCl_3 , δ , ppm): 3.92 (s, 6H, methoxy H_b), 6.91 (d, $J = 8.5$ Hz, 4H, H_j), 6.98 (d, $J = 8.5$ Hz, 2H, H_c), 7.07 (m, 12H, $H_m + H_k$), 7.24 (m, 10H, $H_d + H_i$), 7.38 (d, $J = 8.5$ Hz, 2H, H_e), 7.53 (s, 2H, H_g), 7.65 (d, $J = 9.0$ Hz, 4H, H_l), 7.86 (d, $J = 8.5$ Hz, 2H, H_f),



Structure 2. [Color figure can be viewed in the online issue, which is available at wileyonlinelibrary.com.]

7.88 (s, 1H, H_a), 8.24 (s, 1H, H_n), 8.61 (s, 2H, amide H_o), 9.32 (s, 1H, amide H_n). Anal. Calcd for C₆₅H₅₀N₆O₅ (995.15): C, 78.45%; H, 5.06%; N, 8.44%. Found: C, 78.25%; H, 4.95%; N, 8.32%.

Preparation of Polymer Films

The electrochemical polymerization experiments were carried out with a CH Instruments 750A electrochemical analyzer. The polymers were synthesized from the acetonitrile solution containing 1.0×10^{-4} M monomers **5** or **5-MeO** and 0.1 M Bu₄NClO₄ via cyclic voltammetry repetitive cycling at the scan rate of 50 mV/s for ten cycles. The polymer was deposited onto the surface of the working electrode (ITO/glass surface, polymer films area about 0.8×1.25 cm²), and the film was rinsed with plenty of acetone for the removal of inorganic salts and other organic impurities formed during the process.

Instrumentations

Infrared (IR) spectra were recorded on a Horiba FT-720 FTIR spectrometer. ¹H NMR spectra were measured on a Bruker Avance 500 FT NMR system with tetramethylsilane as an internal standard. Elemental analyses were run in a Heraeus Vario EL III CHNS elemental analyzer. Ultraviolet-visible (UV-vis) spectra of the polymer films were recorded on an Agilent 8453 UV-Visible spectrometer. The absorption spectra of monomer and polymers were recorded in CH₂Cl₂ solution or as solid films on ITO/glass substrate. The optical bandgaps (E_g) of the monomers and polymers were calculated from their absorption edges. Photoluminescence (PL) spectra were measured with a Varian Cary Eclipse fluorescence spectrophotometer. Fluorescence quantum yields (Φ_F) of the samples in different solvent were measured by using quinine sulfate in 1 N H₂SO₄ as a reference standard ($\Phi_F = 54.6\%$). All corrected fluorescence excitation spectra were found to be equivalent to their respective absorption spectra. Electrochemistry was performed with a CHI 750A electrochemical analyzer. Cyclic voltammetry was conducted with the use of a three-electrode cell in which ITO (polymer films area about 0.8×1.25 cm²) was used as a working electrode. A platinum wire was used as an auxiliary

electrode. All cell potentials were taken with the use of an Ag/AgCl reference electrode. Ferrocene was used as an external reference for calibration (+0.48 V vs. Ag/AgCl). Spectroelectrochemical experiments were carried out in a cell built from a commercial UV-vis cuvette using an Agilent 8453 UV-vis diode array spectrophotometer. The cell was composed of a 1-cm cuvette, ITO as a working electrode, a platinum wire as an auxiliary electrode, and an Ag/AgCl reference electrode.

RESULTS AND DISCUSSION

Monomer Synthesis

The TPA and carbazole-capped star-shaped monomers, **5** and **5-MeO**, were prepared by the synthetic route outlined in Scheme 1. In the first step, the intermediate compounds, *N*-(4-aminophenyl)carbazole (**2**) and 3,6-dimethoxy-9-(4-aminophenyl)carbazole (**2-MeO**) were prepared by the CsF-mediated nucleophilic displacement reaction of carbazole

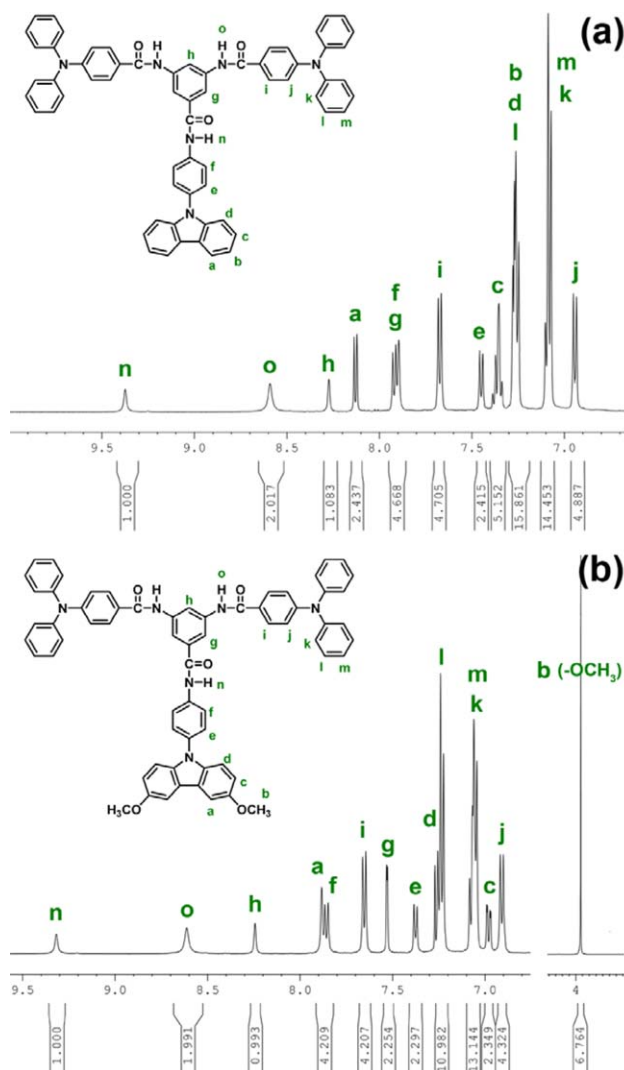


FIGURE 2 ¹H NMR spectra of monomers (a) **5** and (b) **5-MeO** in CDCl₃. [Color figure can be viewed in the online issue, which is available at wileyonlinelibrary.com.]

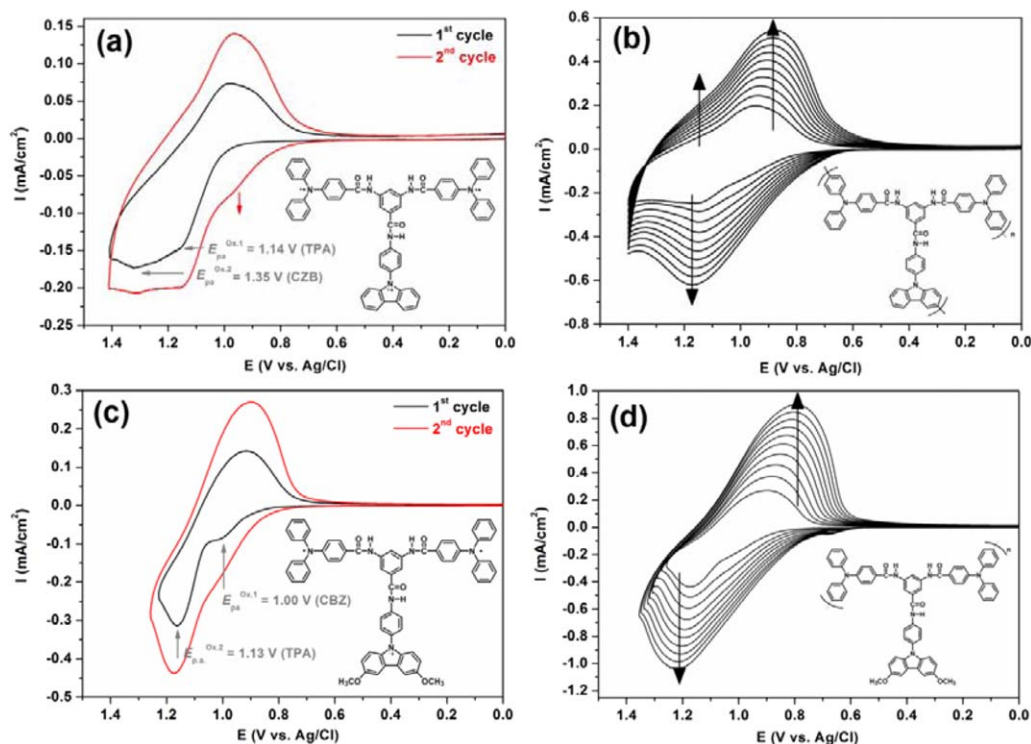


FIGURE 3 Cyclic voltammograms and repeated potential scanning of **5** and **5-MeO** with a scan rate of 50 mV/s in 0.1 M Bu₄NClO₄/CH₃CN solution. [Color figure can be viewed in the online issue, which is available at wileyonlinelibrary.com.]

and 3,6-dimethoxycarbazole, respectively, with *p*-fluoronitrobenzene, followed by hydrazine Pd/C-catalytic reduction. The intermediate dinitro compounds, *N*-(4-(9H-carbazol-9-yl)phenyl)-3,5-dinitrobenzamide (**3**) and *N*-[4-(3,6-dimethoxycarbazol-9-yl)phenyl]-3,5-dinitrobenzamide (**3-MeO**) were prepared by condensation of **2** and **2-MeO**, respectively, with 3,5-dinitrobenzoyl chloride. Reduction of the nitro group of compound **3** and **3-MeO** by means of hydrazine and Pd/C

gave *N*-(4-(carbazol-9-yl)phenyl)-3,5-diaminobenzamide (**4**) and *N*-[4-(3,6-dimethoxycarbazol-9-yl)phenyl]-3,5-diaminobenzamide (**4-MeO**), respectively. The synthetic details and the characterization data of diamino compounds **4** and **4-MeO** were reported previously.²³ The target star-shaped monomers **5** and **5-MeO** were synthesized from **4** and **4-MeO**, respectively, with 4-carboxytriphenylamine using triphenyl phosphite (TPP) and pyridine as condensing agents.

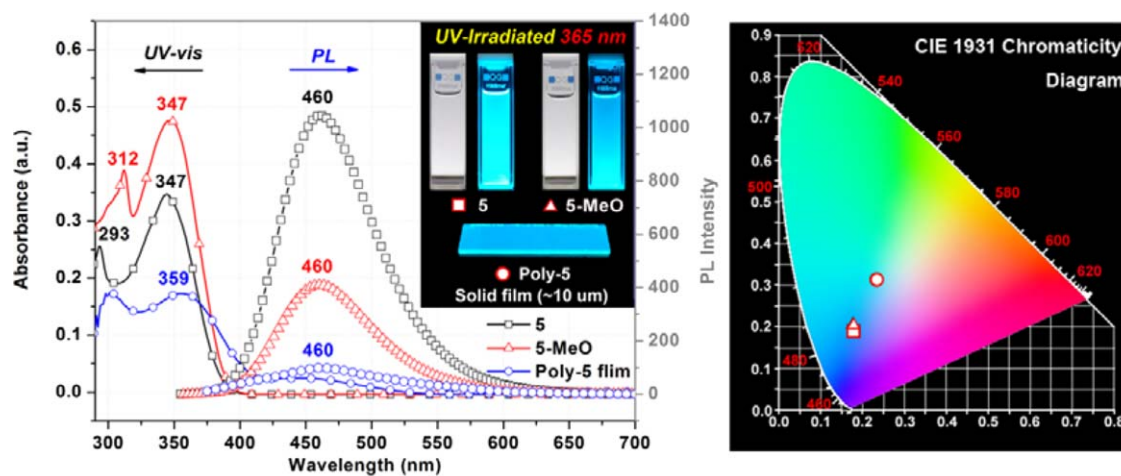


FIGURE 4 UV-vis absorption and PL spectra of the dilute solutions of **5** and **5-MeO** in CH₂Cl₂ (1 × 10⁻⁵ M) and the thin film of **Poly-5**. Photos show the PL images of the solutions of monomers and the **Poly-5** film upon UV exposure (excited at 365 nm). [Color figure can be viewed in the online issue, which is available at wileyonlinelibrary.com.]

TABLE 1 Optical Properties of Monomers and Polymers

Monomer	CH ₂ Cl ₂ (1 × 10 ⁻⁵ M) Solution				
	$\lambda_{\max}^{\text{abs}}$ (nm)	$\lambda_{\max}^{\text{PL}}$ (nm)	Φ_{PL} (%) ^a	CIE 1931	
				X	Y
5	293, 347	460	42.6	0.171	0.198
5-MeO	312, 347	460	25.2	0.171	0.203
Polymer	Film (~10 μm)				
	$\lambda_{\max}^{\text{abs}}$ (nm)	$\lambda_{\max}^{\text{PL}}$ (nm)	$\lambda_{\text{onset}}^{\text{abs}}$ (nm)	CIE 1931	
				X	Y
Poly-5	312, 359	460	413	0.233	0.311
Poly-5-MeO	312, 361	– ^b	420	–	–

^a The fluorescent quantum yield was calculated in an integrating sphere with quinine sulfate as the standard ($\Phi_{\text{PL}} = 54.6\%$).

^b Difficult to define.

IR, ¹H NMR, and ¹³C NMR spectroscopic techniques were used to identify structures of the intermediate compounds and the target monomers.

Figure 1 illustrates FTIR spectra of the synthesized compounds **3–5** and **3-MeO** to **5-MeO**. The IR spectra of compounds **3** and **3-MeO** gave characteristic bands of nitro groups at around 1547 and 1340 cm⁻¹ (–NO₂ asymmetric and symmetric stretching), which disappeared after reduction. Diamines **4** and **4-MeO** showed a typical –NH₂ stretching absorption pair in the region of 3200–3500 cm⁻¹. After condensation with 4-carboxytriphenylamine, the characteristic absorptions of the primary amino group disappeared. The IR spectra of **5** and **5-MeO** showed the characteristic amide absorption bands at around 3300 cm⁻¹ (N–H stretching) and 1650 cm⁻¹ (amide carbonyl stretching). Figure 2 illustrates the high-resolution proton NMR spectra of **5** and **5-MeO** in CDCl₃, and the spectra agree well with their proposed molecular structures.

Preparation of Polymer Films

All electrochemical polymerization processes of monomers were performed on the ITO glass slides in a reaction medium containing 10⁻⁴ M monomer and 0.1 M Bu₄NClO₄ in acetonitrile via repetitive cycling at a potential scan rate of 50 mV/s. Figure 3(a) displays the first two consecutive CV scans of **5**. For the first positive potential scan, we observe two overlapped oxidation waves at about 1.14 and 1.35 V, respectively. It is known that TPA and CBZ moieties can be oxidized to the respective mono radical cations and that CBZ is oxidized at a potential higher than that of the structurally related TPA.^{16,19} Thus, we propose that the TPA groups of monomer **5** are involved in the first oxidation process and the CBZ group is involved in the second oxidation process. In the second scan, a new oxidation peak appeared at a lower potential of 0.95 V, which might be associated with the first oxidation process of tetraphenylbenzidine (TPB), biscarbazole, or the mixed TPA-carbazole structure. As shown in Figure 3(b), upon repetitive scanning of the solution of **5** over the voltage range from 0 to 1.4 V, new redox

patterns were found to grow in intensity on the electrode. The increase of redox current densities by successive CV scans indicates the formation of the electrochemically active polymeric film on the electrode surface. After being immersed in water for a certain period, a polymer film could be removed from the ITO-glass surface. The electrodeposited film of monomer **5** (coded with **Poly-5**) is proposed to possess a crosslinked polymer structure formed by the possible TPA-TPA, carbazole-carbazole, and TPA-carbazole coupling reactions. As shown in Figure 3(c), monomer **5-MeO** shows two distinguishable oxidation waves in the first CV scan. The first oxidation wave at $E_{\text{pa}} = 1.00$ V appears to involve one electron loss from the 3,6-dimethoxycarbazole unit, and the second oxidation wave at $E_{\text{pa}} = 1.13$ V is related to the electron losses from the TPA unit. The decrease in oxidation potential of the carbazole unit is apparently attributable to the introduction of electron-donating methoxy groups on its C-3 and C-6 positions. As the CV scan continued [Fig. 3(d)], the increase in the redox wave current densities implied that the amount of electroactive polymer deposited on the electrode was increasing. The structure of the polymer (**Poly-5-MeO**) electropolymerized from monomer **5-MeO** is suggested to be linear in large part because the electroactive sites of the carbazole unit are blocked with methoxy groups

TABLE 2 Optical Properties of Monomers and Polymers

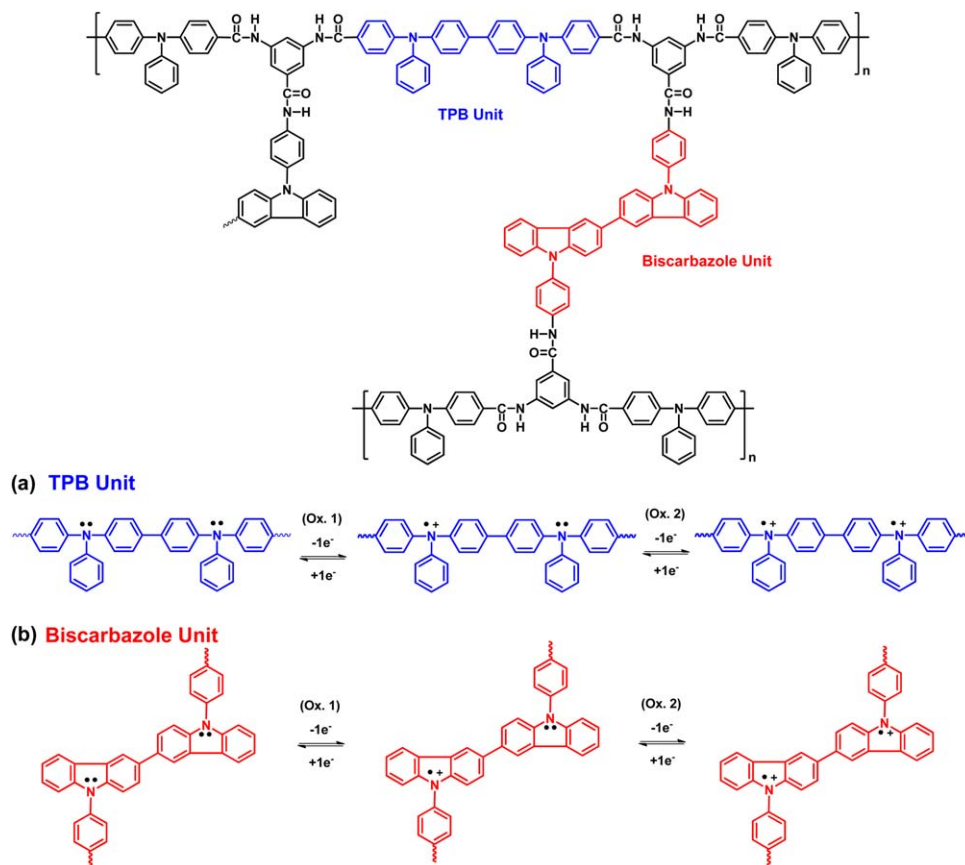
Molecules	Oxidation Potential (V) ^a		$E_{\text{g}}^{\text{opt}}$ (eV) ^b	Energy Levels (eV) ^c	
	E_{onset}	$E_{1/2}$		HOMO	LUMO
5	1.01	1.13, 1.24	3.10	5.37	2.29
5-MeO	0.88	1.00, 1.13	3.09	5.24	2.15
Poly-5	0.75	1.17	3.00	5.11	2.11
Poly-5-MeO	0.77	1.20	2.95	5.13	2.18

^a vs. Ag/AgCl in CH₃CN.

^b Optical bandgap, derived from the optical absorption edge;

$E_{\text{g}}^{\text{opt}} = 1240/\lambda_{\text{onset}}$.

^c $E_{\text{HOMO}} = -(E_{\text{onset}} + 4.8)$ (eV); $E_{\text{LUMO}} = E_{\text{HOMO}} - E_{\text{g}}^{\text{opt}}$.



SCHEME 2 Anodic oxidation pathways of (a) TPB and (b) biscarbazole units. [Color figure can be viewed in the online issue, which is available at wileyonlinelibrary.com.]

and the polymer is mainly built up via the TPA-TPA coupling reactions.

Absorption and Fluorescence Properties

All the monomers and polymers were examined by UV-vis absorption and photoluminescence (PL) spectroscopy. Figure 4 shows the absorption and emission profiles of the monomers and polymers, together with their PL images on exposure to an UV light in both solution and solid states. The

relevant absorption and PL data are collected in Table 1. The dilute solutions in CH_2Cl_2 of monomers **5** and **5-MeO** exhibited two UV-vis absorption peaks at 293–312 and 347 nm, assignable to the $\pi-\pi^*$ and $n-\pi^*$ transitions of the carbazole and TPA moieties. The solutions of monomers **5** and **5-MeO** exhibited blue emission at the maximum peaks of 460 nm with PL quantum yield of 42.6% and 25.2%, respectively. The lower Φ_{PL} of monomer **5-MeO** may be attributed to increased energy dissipation during the excited-state lifetime

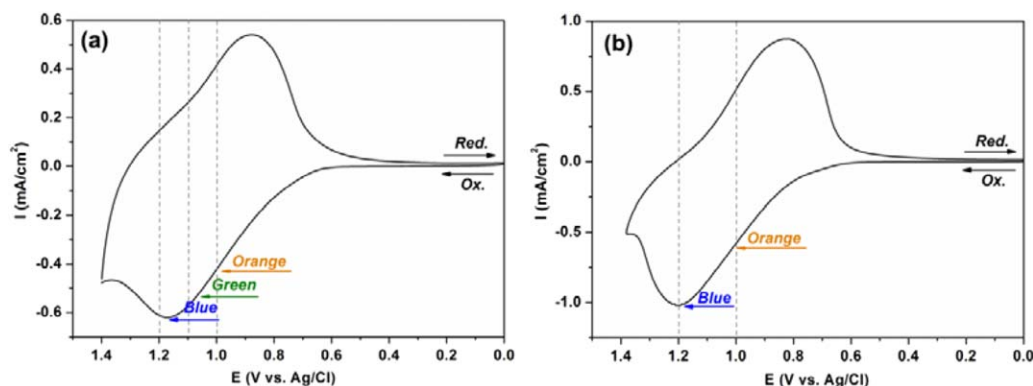


FIGURE 5 Cyclic voltammograms of (a) **Poly-5** and (b) **Poly-5-MeO** polymer films on the ITO-coated glass slide in 0.1 M $\text{Bu}_4\text{NClO}_4/\text{CH}_3\text{CN}$ at a scan rate of 50 mV/s. [Color figure can be viewed in the online issue, which is available at wileyonlinelibrary.com.]

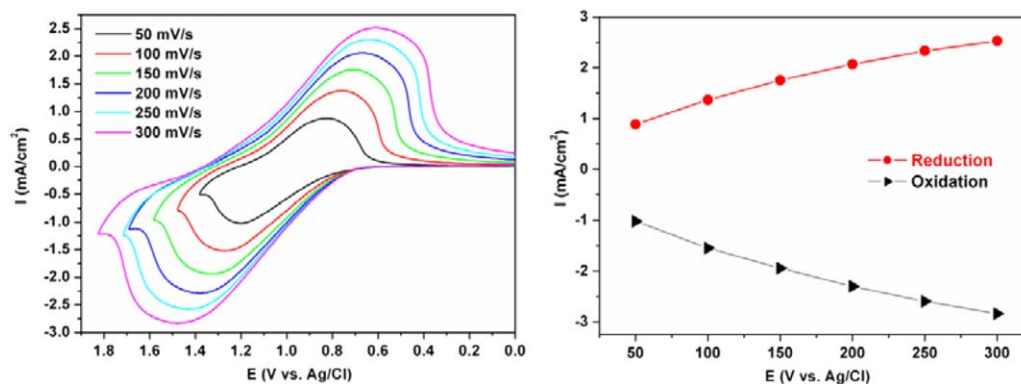


FIGURE 6 Scan rate dependence of **Poly-5-MeO** film on ITO/glass surface in 0.1 M $\text{Bu}_4\text{NClO}_4/\text{CH}_3\text{CN}$ solution at different scan rates between 50 and 300 mV/s. [Color figure can be viewed in the online issue, which is available at wileyonlinelibrary.com.]

caused by the conformational changes of the methoxy groups. Solid film absorption spectra of the polymers were similar to those in solution, with a slight red-shift of ca. 12–14 nm. As shown in the inset of Figure 4, the electrodepos-

ited film of **Poly-5** displayed a strong blue emission upon exposure to UV irradiation. The absorption onsets of the polymer films of **Poly-5** and **Poly-5-MeO** were recorded at 413 and 420 nm, respectively, which correspond to bandgaps of 3.00 and 2.95 eV, respectively.

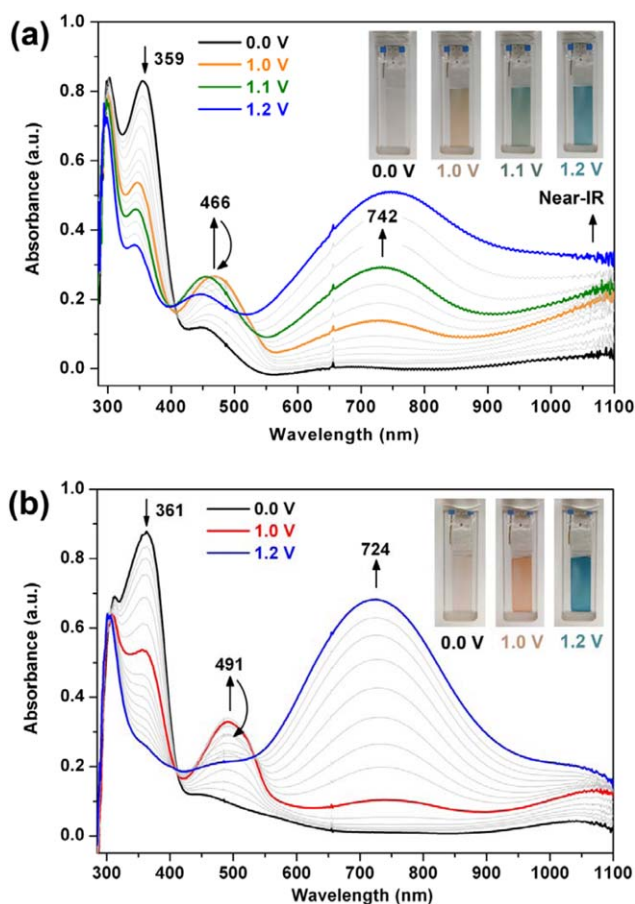


FIGURE 7 Spectroelectrochemical measurements and color changes of (a) **Poly-5** and (b) **Poly-5-MeO** film on an ITO-coated glass in 0.1 M $\text{Bu}_4\text{NClO}_4/\text{CH}_3\text{CN}$ at various applied potentials (vs. Ag/AgCl). [Color figure can be viewed in the online issue, which is available at wileyonlinelibrary.com.]

Electrochemical Properties of the Electrodeposited Films

The electrochemical behavior of the electrodeposited polymer films **Poly-5** and **Poly-5-MeO** was investigated by cyclic voltammetry in a monomer-free $\text{Bu}_4\text{NClO}_4/\text{CH}_3\text{CN}$ solution. The quantitative details are summarized in Table 2. As shown in Figure 5, both of the **Poly-5** and **Poly-5-MeO** films showed only one broad oxidation peak, although two oxidation processes of the TBP and biscarbazole moiety were expected (Scheme 2). The half-wave potentials ($E_{1/2}$) of **Poly-5** and **Poly-5-MeO** were read at 1.17 and 1.20 V, respectively. Figure 6 shows the electrochemical behavior of the **Poly-5-MeO** films at different scan rates between 50 and 300 mV/s in 0.1 M $\text{Bu}_4\text{NClO}_4/\text{CH}_3\text{CN}$. A linear dependence of the peak currents as a function of scan rates indicated that the electrochemical processes are reversible and not diffusion limited, and the electroactive polymer is well adhered to the working electrode (ITO glass) surface.

The highest occupied molecular orbital (HOMO) and lowest unoccupied molecular orbital (LUMO) energy levels of the investigated polymers were estimated from the E_{onset} values. Assuming that the HOMO energy level for the ferrocene/ferrocenium (Fc/Fc^+) standard is 4.80 eV with respect to the zero vacuum level, the HOMO levels for **Poly-5** and **Poly-5-MeO** were calculated to be 5.11 and 5.13 eV (relative to the vacuum energy level), respectively. Their LUMO energy levels deduced from the bandgap calculated from the optical absorption edge were 2.11 and 2.18 eV, respectively (Table 2). According to the HOMO and LUMO energy levels obtained, the electro-generated polymer films in this study might be used as hole injection and transport materials.

Spectroelectrochemical and Electrochromic Properties

Spectroelectrochemistry were performed on the electro-generated polymeric films on ITO glass to clarify its

electronic structure and optical behavior upon oxidation. UV-vis-NIR absorbance curves correlated to applied potentials of the **Poly-5** and **Poly-5-MeO** films are presented in Figure 7(a,b), respectively. In the neutral state, **Poly-5** exhibited strong absorption at wavelength 312 and 359 nm, characteristic for π - π^* transition band of the polymer, but it was almost transparent in the visible region and NIR regions. Upon oxidation (increasing applied voltage from 0.00 to 1.00 V), the absorption of π - π^* transition at 359 nm gradually decreased while two new absorption peaks at 446 and 742 nm and a broadband from 900 nm extended to the NIR region grew up. We attribute this spectral change to the formation of polarons of **Poly-5** caused by the first oxidation of the possible TPB, biscarbazole, and TPA-carbazole units. The absorption band in the NIR region may be attributed to an intervalence charge transfer (IVCT) between states in which the positive charge is centered at different amino centers (TPB, biscarbazole, or TPA-carbazole). The IVCT phenomenon of the family of triarylamines with multiple amino centers has been reported in literature.²⁵ During the first oxidation process the color of the polymer film changed from colorless to pale orange. When the applied potential was increased stepwise to 1.20 V, the absorption band at 446 nm decreased gradually and the absorption band at 742 nm increased in intensity. The spectral change can be attributed to the formation of bipolarons of the polymer (Scheme 2). Apparent color changes (from pale orange, via green, to blue) could be observed during the second oxidation process. The observed spectral changes of the **Poly-5** film were fully reversible upon varying the applied potential. Upon oxidation, the **Poly-5-MeO** film showed similar spectral changes. However, the fully oxidized form of this polymer revealed a strong absorption at 724 nm while a decreased absorption intensity in the NIR region. The decrease in NIR absorption may be explained by the lack of biscarbazole units in this polymer. The bathochromic shift in the visible and NIR ranges may indicate that a more stable charged moiety is present in the film structure of **Poly-5**²⁺ due to the planar biscarbazole unit.

CONCLUSIONS

Two star-shaped monomers **5** and **5-MeO** were synthesized and characterized. These two monomers are electrochemically active and can be electropolymerized into robust polymer films on the electrode surface via electrochemical oxidative coupling of arylamino groups. The electrodeposited polymer films showed moderate blue fluorescence and exhibited reversible electrochemical oxidation processes in the potential range of 0–1.4 V. Both films showed multielectrochromic behavior, exhibiting almost transparent colorless, pale orange and blue colors, according to their oxidation state. The polymer film from monomer **5** reveals an enhanced NIR absorption at its oxidized state as compared to the corresponding one from monomer **5-MeO**. This work provides a model to design star-shaped monomers capable to form electrochemically active polymers with potential applications in electronic and optoelectronic devices.

ACKNOWLEDGMENT

The authors thank the Ministry of Science and Technology of Taiwan for the financial support.

REFERENCES AND NOTES

- 1 P. M. S. Monk, R. J. Mortimer, D. R. Rosseinsky, *Electrochromism and Electrochromic Devices*; Cambridge University Press: Cambridge, UK, **2007**.
- 2 (a) R. Baetens, B. P. Jelle, A. Gustavsen, *Sol. Energy Mater. Sol. Cells* **2010**, *94*, 87–105; (b) C. G. Granqvist, *Thin Solid Films* **2014**, *564*, 1–38.
- 3 (a) C. Ma, M. Taya, C. Xu, *Polym. Eng. Sci.* **2008**, *48*, 2224–2228; (b) A. M. Osterholm, D. E. Shen, J. A. Kerszulis, R. H. Bulloch, M. Kuepfert, A. L. Dyer, J. R. Reynolds, *ACS Appl. Mater. Interfaces* **2015**, *7*, 1413–1421.
- 4 (a) R. J. Mortimer, A. L. Dyer, J. R. Reynolds, *Displays* **2006**, *27*, 2–18; (b) P. M. Beaujuge, S. Ellinger, J. R. Reynolds, *Nat. Mater.* **2008**, *7*, 795–799.
- 5 S. Beaupre, A. C. Breton, J. Dumas, M. Leclerc, *Chem. Mater.* **2009**, *21*, 1504–1513.
- 6 www.gentex.com (accessed: January 2016).
- 7 (a) D. R. Rosseinsky, R. J. Mortimer, *Adv. Mater.* **2001**, *13*, 783–793; (b) F. S. Han, M. Higuchi, D. G. Kurth, *J. Am. Chem. Soc.* **2008**, *130*, 2073–2081; (c) A. Maier, A. R. Rabindranath, B. Tieke, *Adv. Mater.* **2009**, *21*, 956–963; (d) A. Patra, M. Bendikov, *J. Mater. Chem.* **2010**, *20*, 422–433; (e) D. T. Gillapie, R. C. Tenent, A. C. Dillon, *J. Mater. Chem.* **2010**, *20*, 9585–9592; (f) R. J. Mortimer, *Annu. Rev. Mater. Res.* **2011**, *41*, 241–268. (g) M. I. Ozkut, S. Atak, A. M. Onal, A. Cihaner, *J. Mater. Chem.* **2011**, *21*, 5268–5272; (h) C.-J. Yao, Y.-W. Zhong, J. N. Yao, *Inorg. Chem.* **2013**, *52*, 10000–10008; (i) E. Karabiyik, E. Sefer, F. Baycan Koyuncu, M. Tonga, E. Ozdemir, S. Koyuncu, *Macromolecules* **2014**, *47*, 8578–8584.
- 8 (a) P. M. Beaujuge, J. R. Reynolds, *Chem. Rev.* **2010**, *110*, 268–320; (b) C. M. Amb, A. L. Dyer, J. R. Reynolds, *Chem. Mater.* **2011**, *23*, 394–415; (c) A. L. Dyer, E. J. Thompson, J. R. Reynolds, *ACS Appl. Mater. Interfaces* **2011**, *3*, 1787–1795; (d) G. Gunbas, L. Toppare, *Chem. Commun.* **2012**, *48*, 1083–1101; (e) J. Jensen, M. Hosel, A. L. Dyer, F. C. Krebs, *Adv. Funct. Mater.* **2015**, *25*, 2073–2090.
- 9 (a) Y. Shirota, *J. Mater. Chem.* **2000**, *10*, 1–25; (b) Z. J. Ning, H. Tian, *Chem. Commun.* **2009**, 5483–5495; (c) M. Liang, J. Chen, *Chem. Soc. Rev.* **2013**, *42*, 3453–3488.
- 10 (a) Y. Shirota, *J. Mater. Chem.* **2005**, *15*, 75–93; (b) Y. Shirota, H. Kageyama, *Chem. Rev.* **2007**, *107*, 953–1010.
- 11 (a) M. Thelakkat, *Macromol. Mater. Eng.* **2002**, *287*, 442–461; (b) A. Iwan, D. Sek, *Prog. Polym. Sci.* **2011**, *36*, 1277–1325.
- 12 T. Janoschka, M. D. Hager, U. S. Schubert, *Adv. Mater.* **2012**, *24*, 6397–6409.
- 13 J. K. Feng, Y. L. Cao, X. P. Ai, H. X. Yang, *J. Power Sources* **2008**, *177*, 199–204.
- 14 M. Yao, H. Senoh, T. Sakai, T. Kiyobayashi, *J. Power Sources* **2012**, *202*, 364–368.
- 15 (a) S.-H. Cheng, S.-H. Hsiao, T.-H. Su, G.-S. Liou, *Macromolecules* **2005**, *38*, 307–316; (b) C.-W. Chang, G.-S. Liou, S.-H. Hsiao, *J. Mater. Chem.* **2007**, *17*, 1007–1015; (c) S.-H. Hsiao, G.-S. Liou, Y.-C. Kung, H.-J. Yen, *Macromolecules* **2008**, *41*, 2800–2808; (d) S.-H. Hsiao, G.-S. Liou, H.-M. Wang, *J. Polym. Sci. Part A: Polym. Chem.* **2009**, *47*, 2330–2343; (e) Y.-C. Kung, S.-H. Hsiao, *J. Mater. Chem.* **2010**, *20*, 5481–5492; (f) Y.-C. Kung, S.-H. Hsiao, *J. Mater. Chem.* **2011**, *21*, 1746–1754; (g) H.-J. Yen,

- G.-S. Liou, *Polym. Chem.* **2012**, *3*, 255–264; (h) S.-H. Hsiao, H.-M. Wang, P.-C. Chang, Y.-R. Kung, T.-M. Lee, *J. Polym. Sci. Part A: Polym. Chem.* **2013**, *51*, 2925–2938; (i) H.-J. Yen, C.-J. Chen, G.-S. Liou, *Adv. Funct. Mater.* **2013**, *23*, 5307–5316; (j) H.-M. Wang, S.-H. Hsiao, *J. Polym. Sci. Part A: Polym. Chem.* **2014**, *52*, 272–286; (k) S.-H. Hsiao, S.-L. Cheng, *J. Polym. Sci. Part A: Polym. Chem.* **2015**, *53*, 496–510; (l) Y. Q. Wang, Y. Liang, J. Y. Zhu, X. D. Bai, X. K. Jiang, Q. Zhang, H. J. Niu, *RSC Adv.* **2015**, *5*, 11071–11076.
- 16** (a) E. T. Seo, R. F. Nelson, J. M. Fritsch, L. S. Marcoux, D. W. Leedy, R. N. Adams, *J. Am. Chem. Soc.* **1966**, *88*, 3498–3503; (b) R. F. Nelson, R. N. Adams, *J. Am. Chem. Soc.* **1968**, *90*, 3925–3930; (c) S. C. Creason, J. Wheeler, R. F. Nelson, *J. Org. Chem.* **1972**, *37*, 4440–4446.
- 17** M. Leung, M. Y. Chou, Y. O. Su, C. L. Chiang, H. L. Chen, C. F. Yang, C. C. Yang, C. C. Lin, H. T. Chen. *Org. Lett.* **2003**, *5*, 839–842.
- 18** (a) J. Natera, L. Otero, L. Sereno, F. Fungo, N. S. Wang, Y.-M. Tsai, T.-Y. Hwu, K.-T. Wong, *Macromolecules* **2007**, *40*, 4456–4463; (b) C.-C. Chiang, H.-C. Chen, C.-s. Lee, M.-k. Leung, K.-R. Lin, K.-H. Hsieh, *Chem. Mater.* **2008**, *20*, 540–552; (c) J. Natera, L. Otero, F. D’Eramo, L. Sereno, F. Fungo, N.-S. Wang, Y.-M. Tsai, K.-T. Wong, *Macromolecules* **2009**, *42*, 626–635; (d) M. I. Mangione, R. A. Spanevello, A. Rumero, D. Heredia, G. Marzari, L. Fernandez, L. Otero, F. Fungo, *Macromolecules* **2013**, *46*, 4754–4763; (e) S.-H. Hsiao, J.-W. Lin, *Polym. Chem.* **2014**, *5*, 6770–6778.
- 19** (a) J. F. Ambrose, R. F. Nelson, *J. Electrochem. Soc.: Electrochem. Sci.* **1968**, *115*, 1159–1164; (b) J. F. Ambrose, L. L. Carpenter, R. F. Nelson, *J. Electrochem. Soc.: Electrochem. Sci. Technol.* **1975**, *122*, 876–894.
- 20** J. F. Morin, M. Leclerc, D. Ades, A. Siove. *Macromol. Rapid Commun.* **2005**, *26*, 761–778.
- 21** (a) S. Koyuncu, B. Gultekin, C. Zafer, H. Bilgili, M. Can, S. Demic, I. Kaya, S. Icli, *Electrochim. Acta* **2009**, *54*, 5694–5702; (b) O. Usluer, S. Koyuncu, S. Demic, R. A. Janssen, *J. Polym. Sci. Part B: Polym. Phys.* **2011**, *49*, 333–341; (c) S.-H. Hsiao, J.-W. Lin, *Macromol. Chem. Phys.* **2014**, *215*, 1525–1532; (d) S.-H. Hsiao, J.-C. Hsueh, *J. Electroana. Chem.* **2015**, *758*, 100–110; (e) S.-H. Hsiao, S.-W. Lin, *Polym. Chem.* **2016**, *7*, 198–211; (f) S.-H. Hsiao, S.-W. Lin, *J. Mater. Chem. C* **2016**, *4*, 1271–1280.
- 22** M. Ghaemy, R. Alizadeh, H. Behmadi. *Eur. Polym. J.* **2009**, *45*, 3108–3115.
- 23** (a) S.-H. Hsiao, H.-M. Wang, J.-W. Lin, W.-J. Guo, Y.-R. Kung, C.-M. Leu, T.-M. Lee, *Mater. Chem. Phys.* **2013**, *141*, 665–673; (b) S.-H. Hsiao, S.-C. Peng, Y.-R. Kung, C.-M. Leu, T.-M. Lee, *Eur. Polym. J.* **2015**, *73*, 50–64.
- 24** S. H. Hsiao, Y. T. Chiu. *RSC Adv.* **2015**, *5*, 90941–90951.
- 25** C. Lambert, G. Noll. *J. Am. Chem. Soc.* **1999**, *121*, 8434–8442.